Solution Processable P3HT/CdS Photodiodes and Their Electrical Characterization

S. Meraz-Dávila, I. Chávez-Urbiola, C.E. Pérez-García, A. Sánchez-Martínez, S.A. Campos-Montiel, C.G. Alvarado-Beltrán, Y.V. Vorobiev and R. Ramírez-Bon[*]

Centro de Investigación y de Estudios Avanzados del IPN. Unidad Querétaro Apdo. Postal 1-798, 76001, Querétaro, Qro., México
[*]E-mail: rrbon@cinvestav.mx

In this work we apply simple layer solution deposition methods for the assembling of CdS/P3HT (poly(3- hexylthiophene)) p-n heterostructures and analyzed their photodetection properties in the visible optical range. The CdS-n layers were deposited on ITO-coated glass substrates by the chemical bath method employing an ammonia-free recipe. The P3HT-p layers were deposited on the CdS/ITO/glass substrates by the casting method from solution by dissolving P3HT in chloroform. As the back electrodes, to complete the p-n heterostructures, carbon (graphite) was used. The electrical properties of the assembled CdS/P3HT hybrid photodiodes in dark and under illumination at several intensities, in the 0-100 mW/cm^2 interval, were analyzed from current density versus voltage (*J-V*) measurements, in the -5V to 5V bias voltage range. From these measurements, the photosensitivity of the photodiodes as a function of bias voltage was determined as 370 mA/W. The response of the photodiodes as a function of illumination intensity was determined from transient photocurrent measurements.

1. INTRODUCTION

Organic semiconductors are nowadays the focus of great research interest. In special, poly(3-hexylthiophene) (P3HT), because of their electronic properties, is suitable for technological applications in a wide range of organic or hybrid devices such as solar cells [1-3], photodiodes [3-7], light-emitting diodes [8-9] and thin film transistors [7,10-12], among others. Organic semiconductors can be organic molecules, oligomers or polymers, and some of the most studied are pentacene [13], poly(3hexylthiophene) (P3HT) [14-15], Phenyl-C61-butyric acid methyl ester (PCBM) [16-17],

Poly(p-phenylene vinylene) (PPV) [18-19], etc. The characteristic structure of these materials is semicrystalline or amorphous, which results in the low charge carrier mobility and short length diffusion of photogenerated carriers. In addition, these organic compounds are unstable when exposed to normal ambient. These drawbacks can be overcome by designing appropriate device configurations and by encapsulation to ensure longer lifetime of the devices, avoiding performance degradation. On the other hand, one of the main advantages of these materials is the easy layer processability, which allows the deposition on large area substrates at low temperature and reduced costs. Typical deposition processes of organic semiconductor layers include casting, spinning and printing [20]. These processes are quite compatible with soft-chemistry processes (sol-gel, chemical bath deposition, electrodeposition, etc.) for the deposition of inorganic semiconductors layers. Therefore, the deposition process compatibility of organic and inorganic layers opens the opportunity to combine them in a wide range of hybrid devices, in which can be exploited in a better way the properties of each material to optimize the device performance.

One of the organic-inorganic hybrid systems that has been widely studied is P3HT-CdS, particularly in CdS/P3HT thin film solar cells. Several configurations of CdS/P3HT solar cells have been reported in literature, taking advantage on the properties and easy processability of both materials. CdS nanoparticles and layers have been used in the different configurations of CdS/P3HT hybrid solar cells [21]. For the case of CdS-n/P3HT-p heterostructured thin film solar cells, there are works of different groups reporting solar cell efficiencies in the range of 0.03-0.44 % [22-23]. In a recent paper [24], we reported the assembling process of CdS/P3HT (poly(3- hexylthiophene)) hybrid solar cells on ITO-coated glass substrates in three different layer configurations: CdS/P3HT bilayer, P3HT-CdS nanoparticles (CdS NPs) hybrid composite layer and CdS/P3HT-CdS NPs bilayer. The CdS window layers were deposited on ITO-coated glass substrates by the chemical bath method employing an ammonia-free recipe [25], meanwhile the P3HT absorbing layers were deposited on the CdS/ITO/Glass substrates by the casting method from solution by dissolving P3HT powder in chloroform.

Conventional p-n heteterojunction are photodiodes, which can be used for the direct detection of light in the different spectral regions, depending on the energy band gaps of the semiconductor layers, mainly that of the absorbent layer. As in the solar cells devices, for this application, the basis for the conversion of light energy into electrical current is the built-in electrical field at the depleted semiconductor p-n interface region, where photogenerated electron-hole pairs are separated. Unlike solar cells, photodiodes operate in reverse bias because the photosensitivity of these devices is much better in this operation mode. Therefore, the application of heterojunction as photodiodes for the light detection is another important option to take advantage on the semiconductor material properties, including organic ones. In this work, we have processed CdS-n/P3HT-p hybrid heterojunctions and analyzed the properties of the photodiodes for light detection in the visible region. It should be noticed that most of the reports on p-n heterostructures for solar cell applications include only characterization for positive bias voltages; therefore, the analysis for the negative voltages is unknown in many cases. This analysis is particularly important to assess the potential application of the p-n heterostructures as photodiode or photosensor. The fabrication of the photodiode devices is very simple and includes two room temperature solution deposition processes: 1) the ammonia-free chemical deposition of the CdS-

n layer and 2) the drop casting of the P3HT-p layer. The substrates for the assembling of the photodiodes were ITO coated glass slides and carbon contacts on the P3HT layer completed the devices. A variant of the chemical bath deposition was used to obtain CdS layers, which employs the incidence of UV light in the reaction solution to promote the layer growth instead of solution heating. To assess the light sensitivity of the CdS-n/P3HT-p assembled photodiodes, *J-V* measurements were performed in dark and under visible light irradiation at several intensities. From these measurements it was determined the photosensitivity of the hybrid photodiodes as a function of bias voltage.

2. EXPERIMENTAL DETAILS

The photodiodes were assembled on ITO-coated glass substrates (2.54 x 2.54 cm^2) by the sequential deposition of the CdS-n and P3HT-p layers, and finally the carbon contacts. The CdS layers were deposited by the chemical bath method employing an ammonia-free recipe [25-27]. The reaction solution was prepared in 100 ml beakers by the sequential addition of 15 ml of 0.05 M CdCl$_2$, 15 ml of 0.5 M C$_6$H$_5$O$_7$Na$_3$ (sodium citrate), 5 ml of 0.5 M KOH, 5 ml of a pH 10 borate buffer,7.5 ml of 0.5 M CS(NH$_2$)$_2$ (thiourea) and 52.5 ml of deionized water. The beaker with the reaction solution at room temperature was placed in a closed box illuminated with a UV lamp (wavelength 265 nm).The substrates immersed in the reaction solution were removed after 5 hours, rinsed with deionized water and dried with nitrogen. For the deposition of the absorbing layers, a solution of 20 mg of P3HT (Aldrich 90%, regio regular) in 1 ml of chloroform was prepared and magnetically stirred for 24 hours at 60 °C in a hot plate. The P3HT layers were deposited on the CdS/ITO/glass substrates by drop casting. For this, several drops of the P3HT solution were poured on the CdS surface and kept at room temperature for 10 min in the hot plate. After deposition, the P3HT/CdS/ITO/glass samples were thermal annealed at 60 °C for 2 hours. Finally, to complete the photodiode hybrid devices, carbon contacts were done on an area of 0.04 cm^2 over the P3HT-player. The carbon contacts were cured at 60°C for 2 hours. The thickness of the CdS and P3HT layers were 90 nm and 2.4 μm, respectively. The transmission (T) and reflection (R) optical spectra of the CdS and P3HT films were measured in the 240-840 nm wavelength range with a Scientific Computing International (SCI) Film Tek ^{TM} 3000 spectrometer. The current density versus voltage (*J-V*) characteristics of the hybrid solar cell structures in darkness and under 20, 40, 60, 80 and 100 mW/cm^2 illumination were measured using a Semiconductor Parameter Analyzer 4155C Agilent in the voltage range from-5 to 5 V in steps of 0.01 V. As the illumination source, a commercial tungsten-halogen lamp was used, which emission spectrum is shown in the inset of Fig. 3. The transient photocurrents (*J-t*, *t*= time) were measured using a 2401 Source Meter Keithey Instrument with a manual pulsed light source (1000 ms) of 20, 40, 60, 80 and 100 mW/cm^2 variable intensity.

3. RESULTS AND DISCUSSION

Figure 1 displays the optical transmission and reflection spectra of the sequential layers deposited on the ITO-coated glass substrate until completing the assembly of the photodiode. The

optical transmission decreases with the number of the different layers deposited on the substrate. The transmission spectra of the ITO/CdS and ITO/CdS/P3HT layers systems show the absorption edge of CdS and P3HT at about 500 (2.5 eV) and 650 nm (1.9 eV), respectively which corresponds to optical transitions at the fundamental absorption band edge of each material. At higher wavelengths, these layers systems have an optical transmission of about 70 and 60 %, respectively. In the later system, the result is interesting because it shows the potential application of the CdS/P3HT heterojunction to form part of a tandem type solar cell. The optical transmittance of the complete photodiode (ITO/CdS/P3HT/C) drops to about 15 % because the absorption of the carbon back contacts. These optical spectra show that the photodiode absorbs light in the 300-650 nm spectral range and therefore is quite appropriate to the detection of light in the visible spectrum range.
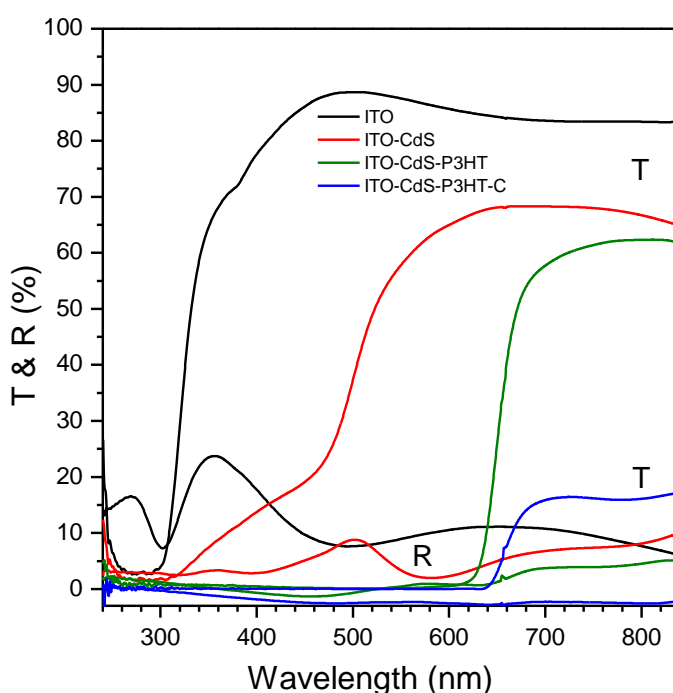

Figure 1. Optical transmission and reflection spectra of the ITO, ITO-CdS, ITO-CdS-P3HT and ITO-CdS-P3HT-C layers systems deposited on glass substrates.

Figure 2 shows the current density-voltage (*J-V*) characteristics of the CdS/P3HT photodiodes measured in dark and under various illumination intensities, from 20 to 100 mW/cm^2. The inset in this figure displays the scheme of the assembled CdS/P3HT photodiode. The *J-V* curve measured in dark shows the current rectification characteristic of diode devices. Under illumination, both, the reverse and forward electrical current density increases as increases the illumination intensity, evidencing the conversion of light energy into electrical current by the photodiode device. The minimum of each *J-V* curve, at around 0 V, shifts to higher voltage with illumination intensity, due to the photovoltaic effect. At this voltage, the current density increases 3 magnitude orders when the photodiode is illuminated with 100 mW/cm^2 intensity. Under illumination, the photogenerated electron-hole pairs are separated more effective at 0 voltage than either at forward or reverse bias. This means that, at this condition, in

the illuminated diode, the electrons are transferred from the valence band to the conduction band resulting in a photocurrent. Also remarkable is the difference of the photocurrents at the different polarizations (reverse bias, forward bias and 0 voltage). Even when at forward voltages the photocurrents are higher compared to the ones measured at reverse bias and 0 voltage, their difference with the curve measured in dark is less than one order of magnitude. On the other hand, at reverse bias and 0 voltage, this difference is of one and three orders of magnitude, respectively. Over all the photodiode presents its higher photosensitivity at 0 voltage for the visible range.
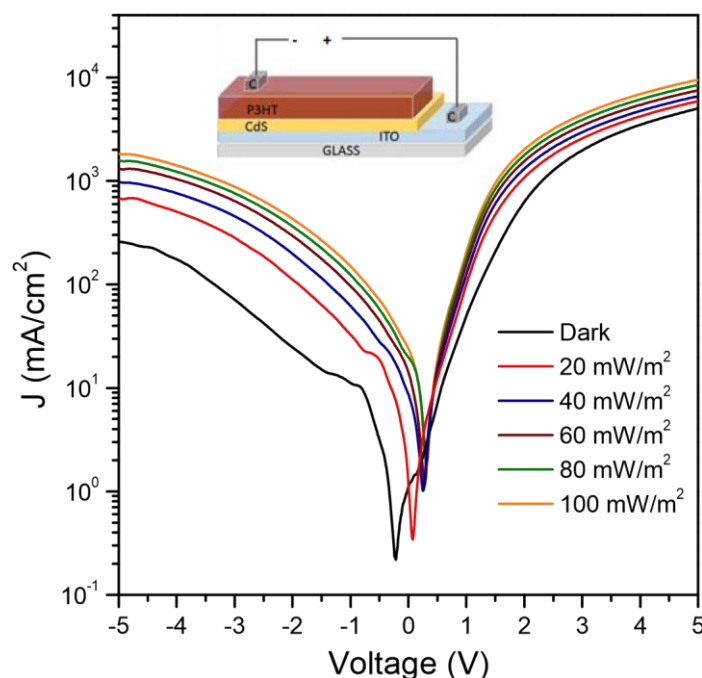

Figure 2. *J* versus *V* measurements in dark and under illumination at several intensities of the assembled P3HT/CdS hybrid photodiodes.

The photosensitivity, *PS(V)=[(J-J$_o$)/J$_o$]·100*, as a function of applied voltage under 100 mW/cm^2 illumination was calculated and the graph is shown in Fig. 3. *Jo* is the current density in dark. The photosensitivity curve displays three relative maxima values at -1.56, 0 and 1.32 V, respectively. As reported in literature, under reverse bias the photodiode has higher photosensitivity than under forward bias, and it is even higher at 0 V. This is because of the difference between dark current and photocurrent generated by the photovoltaic effect. Anyhow, without the photovoltaic effect, the photsensitivity of the device is higher in reverse bias than in the forward bias, which is a typical behavior of photodiodes [3-7]. In Fig. 4 are shown current density pulses (transient photocurrents) measured in the photodiode at 0 V under several illumination intensities. Transient photocurrent measurement is a well-known technique to understand the photoconduction mechanism of any kind of photodiode [28-30]. The current density in dark (off current density) increases immediately when the photodiode is illuminated to values, which increase with illumination intensity (on current density).

The density current pulses are formed when the illumination on the photodiode is turned off and then the current density immediately drops to the off values.
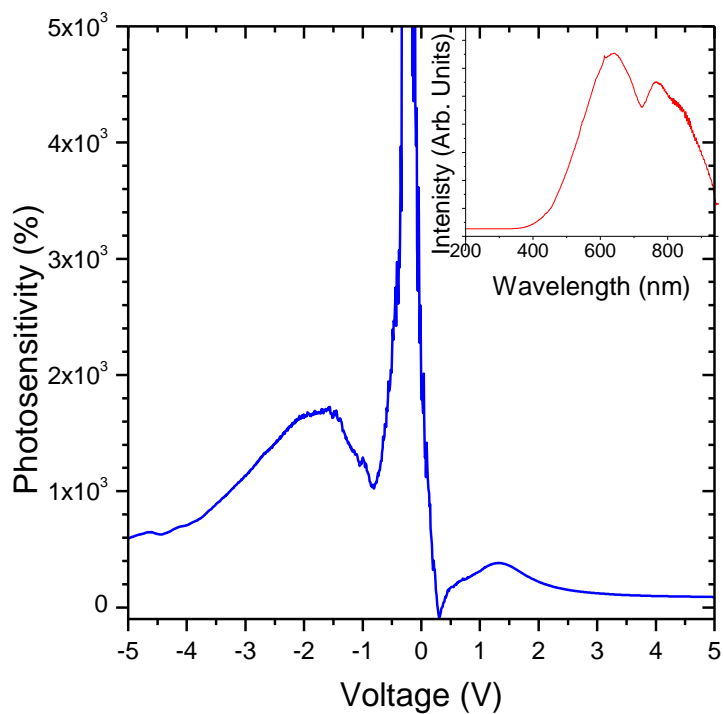

Figure 3. Photosensitivity versus voltage measurement of the P3HT/CdS assembled hybrid photodiode under 100mW/cm^{2}illumination. The inset displays the emission spectrum of the illumination source.
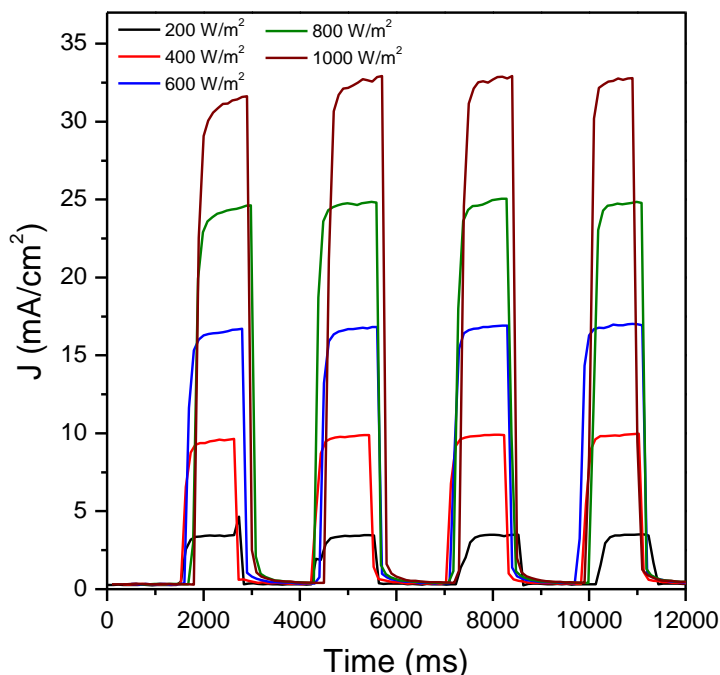

Figure 4. *J* versus *t* measurements of the P3HT/CdS assembled hybrid photodiodes under 100 ms light pulses illumination at several intensities.

As can be seen in this graph, the photodiode has a quite satisfactory on/off response.
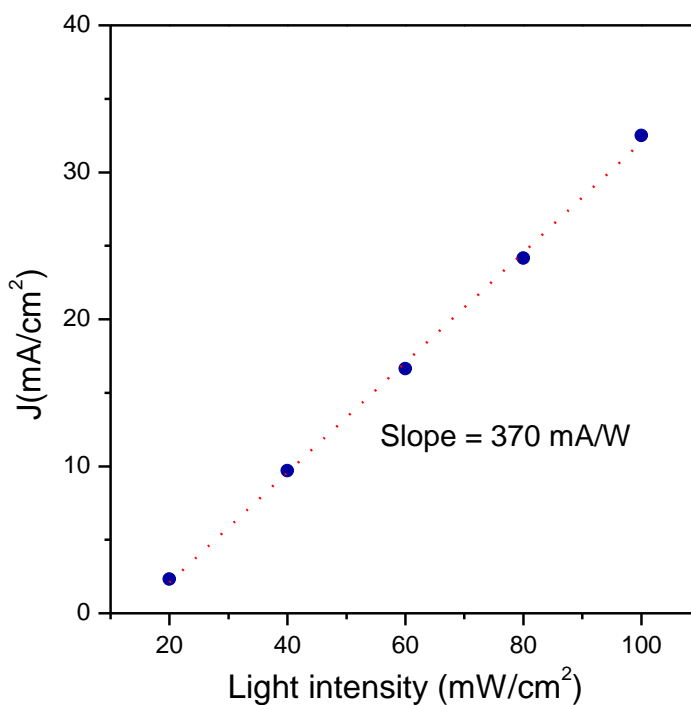

Figure 5. Height of the current density pulses as a function of illumination intensity. The dotted line is the best fit to a straight line, which slope is indicated in the graph.

When the device is illuminated the photogenerated electron-hole pairs increase the free charge producing the observed current density increase. The electrical photocurrent remains constant until illumination is turned off when the free charge drops to the dark values level. Some delay is observed between the time the illumination is turned off and the time when the current returns to the off values. Some charge carriers trapping, which delay the decay of the photocurrent produces this effect.

Figure 5 shows the height of the current density pulses as a function of illumination intensity at 0 V, where it is observed a linear behavior. The experimental data was fit to a straight line, shown as a dotted line in the graph, and the resulting slope was 370 mA/W (photoresponsivity). If we use a well-known expression for estimation of photosensitivity, *PR*,

$$PR = 0.806 \ \eta\lambda$$

where η is the quantum efficiency and λ is the working wavelength in μm, we obtain *PR* = 0.403 taking η = 1 and λ=0.5 μm. Thus, we see that our hybrid photodiode has sensitivity close to ideal one. Similar results are reported literature for P3HT-based phodiodes with different structures (Visible-Near Infra-Red range): P3HT/ZnO nanowires, 310 mA/W at -2V [4], P3HT/(PCBM), 180 mA/W at -6V [31], P3HT/PCBM 177mA/W at -1V [7], PbS-QDs:P3HT:PCBM BH, 130-500 mA/W at -5V [32], CdSe QDs/spiro-TPD, 410-61 mA/W at -300V [33], P3HT/F8TBT, 100 mA/W at -0.5V [34], PTB7:PC$_{71}$BM, 100 mA/W at 2V [35], (PEDOT:PSS)/P3HT:PCBM 360 mA/W at -5V [36]. Since *PR* is a convenient figure of merit to compare the photodiodes performance, according to these reports, the photoresponsivity of the hybrid P3HT/CdS photodiodes is quite satisfactory with the increase of 370 mA of the photocurrent per each irradiation watt. This is rather higher compared to that of purely

organic photodiodes due to the inorganic contribution in our hybrid device. On the other hand, the *PR* of our hybrid devices is similar to that of other hybrid devices.

4. CONCLUSIONS

In this work, we have analyzed the potential applications of organic-inorganic P3HT/CdS heterostructures as photodiodes for light detection in the visible range. The electrical characterization of the hybrid heterostructures in dark and under illumination at several intensities shows proper and convenient photodiode behaviour with good photosensitivity and photoresponsitivity. The response of the hybrid photodiodes under illumination is of 370 mA per watt of illumination intensity, which is comparable to the response of other organic and hybrid photodiodes reported in literature. These results show that hybrid P3HT/CdS photodiodes with adequate photoresponse can be prepared in simple, low temperature, economic and environmentally friendly solution deposition processes.

References

1. N. Ćelić, E. Pavlica, M. Borovšak, J. Strle, J. Buh, J. Zavašnik, G. Bratina, P. Denk, M. Scharber, N. S. Sariciftci, and D. Mihailovic, *Synth. Met.*, 212 (2016) 105.
2. S. R. Gollu, R. Sharma, G. Srinivas, S. Kundu, and D. Gupta, *Org. Electron.*, 29 (2016) 79.
3. P. Peumans, A. Yakimov, and S. R. Forrest, *J. Appl. Phys.*, 104 (2003) 3693.
4. Z. Yuan and Y. Ren, *Phys. E Low-Dimensional Syst. Nanostructures*, 48 (2013) 128.
5. J. M. Cho, D. S. Kim, S. Bae, S.-J. Moon, W. S. Shin, D. H. Kim, S. H. Kim, A. Sperlich, S. Väth, V. Dyakonov, and J.-K. Lee, *Org. Electron.*, 27 (2015) 119.
6. H. Zhang, S. Jenatsch, J. De Jonghe, F. Nüesch, R. Steim, A. C. Véron, and R. Hany, *Sci. Rep.*, 5 (2015) 9439.
7. K.-J. Baeg, M. Binda, D. Natali, M. Caironi, and Y.-Y. Noh, *Adv. Mater.*, 25 (2013) 4267.
8. C. Lee, J. Huang, S. Hsu, W. Su, and C. Lin, Optical Fiber Communication & Optoelectronic Exposition & Conference, 2008. AOE 2008. Asia
9. Z. L. Li, S. C. Yang, H. F. Meng, Y. S. Chen, Y. Z. Yang, C. H. Liu, S. F. Horng, C. S. Hsu, L. C. Chen, J. P. Hu, and R. H. Lee, *Appl. Phys. Lett.*, 84 (2004) 3558.
10. S. Han, X. Zhuang, W. Shi, X. Yang, L. Li, and J. Yu, *Sensors Actuat. B-Chem.*, 225 (2016) 10.
11. H. Chang, P. Wang, H. Li, J. Zhang, and D. Yan, *Synth. Met.*, 184 (2013) 1.
12. M. Yasin, T. Tauqeer, K. S. Karimov, S. E. San, A. Kösemen, Y. Yerli, and A. V. Tunc, *Microelectron. Eng.*, 130 (2014) 13.
13. H. Klauk, S. Member, D. J. Gundlach, S. Member, J. a Nichols, and T. N. Jackson, *IEEE T. Electron. Dev.*, 46 (1999) 1258.
14. D. Chirvase, J. Parisi, J. C. Hummelen, and V. Dyakonov, *Nanotechnology*, 15 (2004) 1317.
15. L. Bian, E. Zhu, J. Tang, W. Tang, and F. Zhang, *Prog. Polym. Sci.*, 37 (2012) 1292.
16. S. A. Jotterand and M. Jobin, *Energy Procedia*, 31 (2013) 117.
17. L. Chang, H. W. a. Lademann, J.-B. Bonekamp, K. Meerholz, and A. J. Moulé, *Adv. Funct. Mater.*, 21 (2011) 1779.

18. S. E. Shaheen, C. J. Brabec, N. S. Sariciftci, F. Padinger, T. Fromherz, and J. C. Hummelen, *Appl. Phys. Lett.*, 78 (2001) 841.
19. J.H. Burroughes, D.D.C. Bradley, A.R. Brown, R.N. Marks, K. Mackay, R.H. Friend, P.L. Burn and A.B. Holmes, *Nature* 347 (1990) 539.
20. F. C. Krebs, *Sol. Energy Mater. Sol. Cells*, 93 (2009) 394.
21. S. Dowland, T. Lutz, A. Ward, S. P. King, A. Sudlow, M. S. Hill, K. C. Molloy, and S. a. Haque, *Adv. Mater.*, 23 (2011) 2739.
22. N. Kumar and V. Dutta, *J. Colloid Interface Sci.*, 434 (2014) 181.
23. H. J. Cortina-Marrero, P. K. Nair, and H. Hu, *Sol. Energy*, 98 (2013) 196.
24. A. Sánchez-Martínez, Y. V Vorobiev, and R. Ramirez-Bon, *Int. J. Electrochem. Sci.*, 10 (2015) 5614.
25. M. G. Sandoval-Paz, M. Sotelo-Lerma, a. Mendoza-Galvan, and R. Ramírez-Bon, *Thin Solid Films*, 515 (2007) 3356.
26. M. G. Sandoval Paz, R. Ramírez Bon. *Thin Solid Films,* 517 (2009) 6747.
27. G. Arreola Jardón, L.A. González, L.A. García-Cerda, B. Gnade, M.A. Quevedo-López, R. Ramírez Bon. *Thin Solid Films,* 519 (2010) 517.
28. F. Yakuphanoglu, F. S. Shokr, R. K. Gupta, A. A. Al-Ghamdi, S. Bin-Omran, Y. Al-Turki, and F. El-Tantawy, *J. Alloys Comp.*, 650 (2015) 671.
29. A. M. Selman, Z. Hassan, M. Husham, and N. M. Ahmed, *Appl. Surf. Sci.*, 305 (2014) 445.
30. A. A. Hendi, *J. Alloys Comp.*, 647 (2015) 259.
31. B. Arredondo, B. Romero, J. Pena, A. Fernández-Pacheco, E. Alonso, R. Vergaz, and C. de Dios, *Sensors*, 13 (2013) 12266.
32. T. Rauch, M. Böberl, S. F. Tedde, J. Fürst, M. V. Kovalenko, G. Hesser, U. Lemmer, W. Heiss, and O. Hayden, *Nat. Photonics*, 3 (2009) 332.
33. T. P. Osedach, S. M. Geyer, J. C. Ho, A. C. Arango, M. G. Bawendi, and V. Bulović, *Appl. Phys. Lett.*, 94 (2009) 043307.
34. P. E. Keivanidis, S.-H. Khong, P. K. H. Ho, N. C. Greenham, and R. H. Friend, *Appl. Phys. Lett.*, 94 (2009) 173303.
35. M. Jahnel, M. Thomschke, S. Ullbrich, K. Fehse, J. D. An, H. Park, K. Leo, C. Im, and V. Kirchhoff, *Microelectron. Eng.*, 152 (2015) 20.
36. S. F. Tedde, J. Kern, T. Sterzl, J. Fu, P. Lugli, and O. Hayden, *Nano Lett.*, 9 (2009) 980.